JOURNAL OF SOLID STATE CHEMISTRY **130,** 184–191 (1997)
ARTICLE NO. SC977278

Topotactic Oxidation of the Quadruple-Rutile-Type Chain Structure $Na_{0.875}Fe_{0.875}Ti_{1.125}O_4$

A. Kuhn,† N. Menéndez,‡ F. García-Alvarado,†,[1] E. Morán,* J. D. Tornero,‡
and M. A. Alario-Franco*

** Departamento de Química Inorgánica, Facultad de Ciencias Químicas, Universidad Complutense de Madrid, 28040 Madrid, Spain; † Departamento de Química Inorgánica y Materiales, Facultad de Ciencias Experimentales y Técnicas, Universidad San Pablo—CEU, 28668 Boadilla del Monte, Madrid, Spain; and ‡ Departamento de Química Física Aplicada, Facultad de Ciencias, Universidad Autónoma de Madrid, 28049 Madrid, Spain*

Received February 26, 1996; in revised form December 30, 1996; accepted January 13, 1997

Sodium removal from $Na_{0.875}Fe_{0.875}Ti_{1.125}O_4$ by means of oxidizing agents leads to the formation of the defect solid solution $Na_{0.875-\delta}Fe_{0.875-\delta}Ti_{1.125}O_4$ ($0 \le \delta \le 0.44$). A systematic increase in the $\underline{a}$ parameter of the orthorhombic unit cell is observed as the sodium content is reduced, while the $\underline{b}$ parameter decreases only slightly. The cell volume remains almost constant as a consequence of the irregular change in the $\underline{c}$ parameter and the different behavior of both the $\underline{a}$ and $\underline{b}$ parameters. Structural changes have been followed by Rietveld powder diffraction analysis. Room- and low-temperature Mössbauer studies confirm the increase in the Fe^{4+} state with decreased sodium content in the less extracted samples with $\delta = 0.10$ and 0.15, whereas a maximum Fe^{4+} content (about 21%) is reached in a sample with $\delta = 0.25$. Surprisingly, the amount of Fe^{4+} does not increase with further sodium extraction. This is thought to be related to the greater oxidative power of the more oxidized materials, which facilitates a subsequent partial backreduction of Fe^{4+} formed during the oxidation procedure. Results of both Mössbauer spectroscopy and structure refinements indicate that the Fe^{4+} cations randomly occupy both octahedral metal positions, $M(1)$ and $M(2)$, of each quadruple rutile unit. © 1997 Academic Press

INTRODUCTION

The crystal structure of the "ferrititanate" $Na_xFe_xTi_{2-x}O_4$ was first reported by Mumme and Reid as a calcium ferrite type (1). The basic unit of the structure (Fig. 1) is a quadruple-rutile chain, in which a pair of edge-shared octahedra, further condensed by edge-sharing to a distorted Z-shaped ribbon, extends along the $\underline{b}$ axis. By sharing four corners, the quadruple-rutile chains leave double tunnels along the $\underline{b}$ axis, which are partially filled by sodium atoms.

As reported in (1), $Na_xFe_xTi_{2-x}O_4$ can sustain different sodium contents. Compounds between $x = 0.75$ and $x = 0.90$ belong to a small region of nonstoichiometric occupancy of the double-barreled tunnels. This is not surprising if one recalls that the $CaFe_2O_4$-type oxides show, very often, nonstoichiometric occupancy of these tunnels. An example is the mixed ferrite $Ca_{1-x/2}(Fe_{2-x}Sn)O_4$ (2), a double-rutile-chain $CaFe_2O_4$-type structure, which can have up to 30% calcium vacancies.

However, other reports claim a unique composition, $Na_xFe_xTi_{2-x}O_4$, with $x = 0.875$ (3). Calcium ferrite-type $NaFeTiO_4$ ($x > 0.875$) and sodium titanate bronze-like $NaFeTi_3O_8$ ($x < 0.875$) were found on each side of the composition $x = 0.875$.

Recently, single crystals of a new sodium titanate, $Na_xTi_2O_4$, were obtained by reaction of sodium metal and titanium oxides at high temperature (4). The homogeneity range of this compound, which is isostructural with $Na_xFe_xTi_{2-x}O_4$, was found to be $0.50 \le x \le 0.57$, showing a large sodium deficiency in the double-tunnel framework.

In a previous paper (5) we reported the synthesis of a new defect solid solution, $Na_{0.875-\delta}Fe_{0.875}Ti_{1.125}O_4$ ($0 \le \delta \le 0.40$), by low-temperature "soft-chemistry" routes. A preliminary characterization was also presented. A significant result of that work was the preparation of samples within a larger nonstoichiometric range. The present paper describes studies of the influence of sodium content in the "$Na_{0.875-\delta}Fe_{0.875}Ti_{1.125}O_4$" structure in different samples ($\delta = 0$, 0.10, 0.15, 0.26, 0.30, and 0.44) in the new extended range ($Na_{0.434}Fe_{0.875}Ti_{1.125}O_4$–$Na_{0.875}Fe_{0.875}Ti_{1.125}O_4$) by means of diffraction techniques complemented by Mössbauer spectroscopy and magnetic measurements.

EXPERIMENTAL

The parent compound, $Na_{0.875}Fe_{0.875}Ti_{1.125}O_4$, was prepared by solid state reaction as previously described (1). Finely ground mixtures of Na_2CO_3 and the appropriate amounts of Fe_2O_3 and TiO_2 (rutile) were fired in air to 1000°C for 12 h, quenched in air, ground, and treated again

---

[1] To whom correspondence should be addressed.

0022-4596/97 $25.00

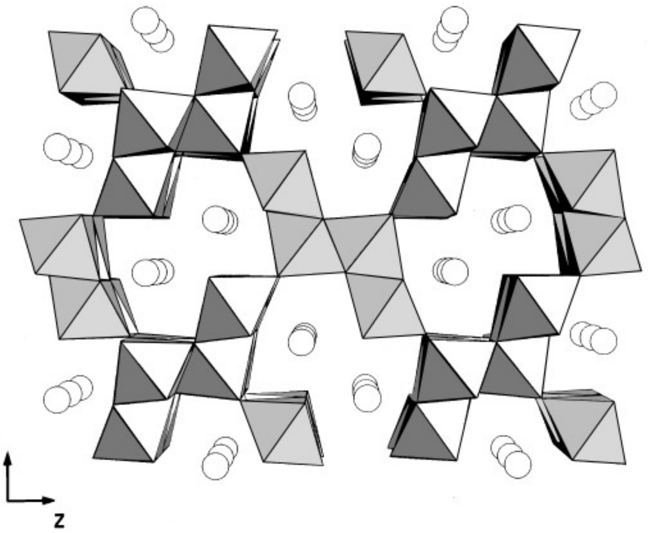

FIG. 1. Projection of the structure of $Na_{0.875-\delta}Fe_{0.875}Ti_{1.125}O_4$ along the tunnel *b* axis.

up to six times at the same temperature with intermediate grindings.

The partial extraction of sodium was achieved at room temperature by soft-chemistry methods. Therefore, the starting material $Na_{0.875}Fe_{0.875}Ti_{1.125}O_4$ was stirred under argon in solutions of dry acetonitrile containing iodine, bromine, or nitronium tetrafluoroborate as oxidant at a 25% excess. Acetonitrile (Aldrich, 99.5%) was first predried with potassium hydroxide to remove most of the water and then fractionally distilled under normal pressure in argon (boiling point, 81°C).

The chemical analysis was performed by inductively coupled plasma (ICP) methods in a calibrated Jovin–Yvon instrument (Model JY-70 plus) as previously reported (5).

X-ray powder diffraction experiments were performed in a Siemens D-5000 apparatus using Cu$K\alpha$ radiation. Silicon was used as internal standard for the determination of the cell parameters. Intensity data were collected at a scan rate of 0.1°/min over a 2θ range from 10° to 65°. For structure refinements, the Rietveld method (6) was applied using the FULLPROF program (7). XRD measurements of oxidized samples were made using an aluminum sample holder, which was loaded in an argon-filled glove box and sealed with a beryllium window.

Magnetic susceptibilities were measured in a DSM-8 DC susceptometer in the temperature range from 4 to 300 K. The calibration was made with ammonium thiocyanate as the standard.

The Mössbauer effect of ^{57}Fe was determined in a conventional spectrometer, and the 77 and 293 K spectra were analyzed using the NORMOS program (8). The velocity and isomer shift scales were calibrated using α-iron metal as the standard.

RESULTS AND DISCUSSION

1. Chemical Oxidation

By exposing the $Na_{0.875}Fe_{0.875}Ti_{1.125}O_4$ powder samples to different oxidation conditions, several compounds $Na_{0.875-\delta}Fe_{0.875}Ti_{1.125}O_4$ $(0 \leq \delta \leq 0.44)$ were obtained. When iodine or bromine was used as the oxidant, sodium extraction was very low, and the δ reached was only 0.02 after 1 week. When nitronium tetrafluoroborate (NO_2BF_4), which possessses a greater oxidative power of 2.1 V vs SHE (standard hydrogen electrode) (9), was employed, an appreciably stronger sodium deficiency was generated in the parent framework. When the starting material was exposed to this stronger oxidant, $\delta = 0.10$ was reached after 2 days. When the oxidation procedure was repeated several times with fresh oxidant in each case, the following amounts of sodium were extracted after 3 days, 5 days, 1 week, and 2 weeks: $\delta = 0.15$, 0.25, 0.30, and 0.44, respectively (see also Table 1). The evolution of the extraction reaction with the strong oxidant NO_2BF_4 as a function of overall time of the consecutive treatments can be seen in Fig. 2. Initially, the sodium extraction reaction proceeds rapidly. The more sodium extracted, the slower further reaction becomes, and the curve finally reaches a plateau. This "saturation" effect is related to the increasing oxidative power of the parent compound with sodium extraction. The maximum possible value of δ, which would correspond to $\delta = 0.875$, i.e., complete removal of Na^+ from the tunnels, was not reached. Following the procedure described in (5), no more than 0.40 Na^+/formula could be extracted. In further oxidation experiments, using prolonged reaction times and treatments with the oxidant NO_2BF_4, we found δ to be 0.44. This value seems then to be the limit of sodium extraction for the NO_2BF_4 oxidation agent, i.e., the removal of 50% of sodium from the framework tunnel structure. Until now, only a few compounds containing Fe^{4+} were known, among which were the earth alkali metal perovskites, e.g., $CaFeO_3$ (10) and $SrFeO_3$ (11). Synthesis of the simple binary oxide FeO_2 has not yet been possible. Sodium extraction from rhombohedral α-$NaFeO_2$ (12) leads to a metastable compound of

TABLE 1
Oxidants Employed and Compositions Obtained from ICP Spectroscopy

Oxidant	Composition obtained	Reaction time	δ per formula
I_2	$Na_{0.875(1)}Fe_{0.874(2)}Ti_{1.124(1)}O_4$	3 days	0.00(1)
Br_2	$Na_{0.850(1)}Fe_{0.875(1)}Ti_{1.121(2)}O_4$	7 days	0.020(1)
NO_2BF_4 (1 ×)	$Na_{0.773(1)}Fe_{0.876(1)}Ti_{1.122(2)}O_4$	2 days	0.102(1)
NO_2BF_4 (2 ×)	$Na_{0.724(3)}Fe_{0.874(1)}Ti_{1.125(1)}O_4$	3 days	0.151(3)
NO_2BF_4 (3 ×)	$Na_{0.620(8)}Fe_{0.875(3)}Ti_{1.123(1)}O_4$	5 days	0.255(8)
NO_2BF_4 (4 ×)	$Na_{0.579(3)}Fe_{0.875(1)}Ti_{1.124(2)}O_4$	7 days	0.296(3)
NO_2BF_4 (5 ×)	$Na_{0.434(1)}Fe_{0.873(1)}Ti_{1.122(2)}O_4$	14 days	0.441(1)

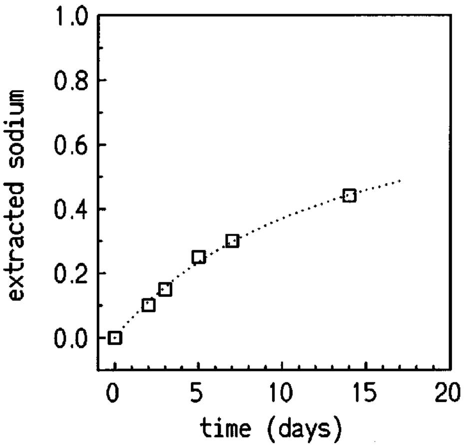

FIG. 2. Amount of extracted sodium δ using NO_2BF_4 as oxidizing agent as a function of overall treatment time. Data were taken from Table 1.

composition $Na_{0.5}FeO_2$ related to the monoclinic $NaMnO_2$-type structure (13). The extraction of all sodium atoms from the parent oxide, $Na_{0.875}Fe_{0.875}Ti_{1.125}O_4$, would produce a compound with the composition $Fe_{0.875}Ti_{1.125}O_4$, in which all Fe would be Fe^{4+}. The existence of this compound seems to be rather complicated, since the stability of Fe as Fe^{3+} is high. Indeed, a compound containing only Fe^{4+} would probably be a very good oxidizing agent! For our powder samples the oxidation reaction was not completed, and the most oxidized specimen had the composition $Na_{0.434(1)}Fe_{0.875(1)}Ti_{1.125(1)}O_{4.0}$. The maximum amount of extracted sodium reached should be enough to produce some detectable structural distortion. The occurrence of such oxidation has been studied by Mössbauer spectroscopy, magnetic measurements, and X-ray diffraction.

2. Characterization of the Oxidized Samples

Mössbauer spectroscopy. Mössbauer spectra were measured to determine the Fe^{4+} state induced by Na extraction. The Mössbauer spectra of $Na_{0.875-\delta}Fe_{0.875}Ti_{1.125}O_4$ ($\delta = 0, 0.10, 0.15, 0.25, 0.30$ and 0.44) at room temperature and 77 K are shown in Figs. 3a and 3b. The corresponding isomer shifts (ISs) and quadrupole splittings (QSs) are listed in Table 2. The spectrum of $Na_{0.875}Fe_{0.875}Ti_{1.125}O_4$ ($\delta = 0$) shows two lines with almost the same intensities corresponding to the Fe^{3+} quadrupole splitting. The values of IS and QS are 0.371(2) and 0.514(4) mm/s at room temperature, whereas at 77 K we obtained 0.482(2) and 0.515(4) mm/s. The isomer shift is appropriate to Fe^{3+}, and the quadrupole splitting indicates that the Fe^{3+} cation is located at asymmetric sites, that is, in an asymmetric octahedral oxygen environment.

The asymmetrical appearance of the spectra for oxidized samples $\delta = 0.10, 0.15, 0.25, 0.30$, and 0.44 as the overlap of two doublets, one from Fe^{3+} and the other from Fe^{4+}, is indicative of the presence of Fe^{4+}. Consideration of this hypothesis yields IS values for Fe^{4+} in good agreement with those of other compounds containing Fe^{4+} (14). The decrease in QS in $Na_{0.875-\delta}Fe_{0.875}Ti_{1.125}O_4$ in the range $0 \leq \delta \leq 0.25$ seems to indicate that the Fe^{3+} environment is made more symmetric by the introduction of Fe^{4+} to the structure, whereas for greater δ values a slight increase in QS can be noted.

The percentages of Fe^{4+} in the samples with $\delta = 0.10$ and 0.15, calculated from the ratio of peak areas in each case, are 10 and 17%, respectively. These values agree fairly well with the amounts deduced from ICP spectroscopy (see Table 2). Since the extraction should be accompanied by oxidation of the solid, we need only consider a change in the oxidation state of one iron cation, from Fe^{III} to Fe^{IV}, for each sodium atom extracted. Therefore, the calculated formula within the sodium deficiency range $0 \leq \delta \leq 0.15$ is $Na_{0.875-\delta}(Fe^{III})_{0.875-\delta}(Fe^{IV})_{\delta}Ti_{1.125}O_{4.0}$, assuming that there are no oxygen vacancies involved in the process. This is supported by results of a single crystal study in which the refinement of the population factors for the oxygen atoms gave no evidence of the existence of oxygen vacancies (15). The spectra of the samples $\delta = 0.10$ and 0.15 show two additional peaks (marked by *), which were determined to correspond to the inner lines of the sextet of unreacted α-Fe_2O_3 during preparation of the starting material (these two oxidized samples had been prepared from a second run of starting material). The concentration of impurities in these samples was determined by Mössbauer spectroscopy to be about 20%. However, α-Fe_2O_3 was not detected by means of X-ray powder diffraction. The lines were verified to be from α-Fe_2O_3 by recording the spectra at a higher Doppler modulation velocity (± 12 mm/s). We obtained $IS = 0.357$ mm/s, $QS = -0.201$ mm/s, and $H = 51.7$ T, which agree fairly well with literature values (14). The percentage of unreacted α-Fe_2O_3 in the samples with $\delta = 0.10$ and 0.15 was taken into account in calculating the Fe^{4+}/Fe^{3+} ratio. This means that the sum of the resonant areas of ^{57}Fe corresponding to the parent compound $Na_{0.875-\delta}Fe_{0.875}Ti_{1.125}O_4$ was set at 100%.

As a surprising result, the amount of Fe^{4+} does not increase, as one would expect, with further sodium extraction, but remains practically constant, as can be easily deduced from Fig. 4. In these more oxidized samples, the amount of Fe^{4+} present in the structure is clearly lower than that expected, and the maximum value for the Fe^{4+}/Fe^{3+} ratio only 0.184 (curve 2). If the extraction–oxidation mechanism fulfills the condition that the extraction of one sodium atom is accompanied by the oxidation of one Fe^{3+} cation to Fe^{4+}, then the Fe^{4+}/Fe^{3+} ratios should be coincident with the δ value for extracted sodium (curve 1).

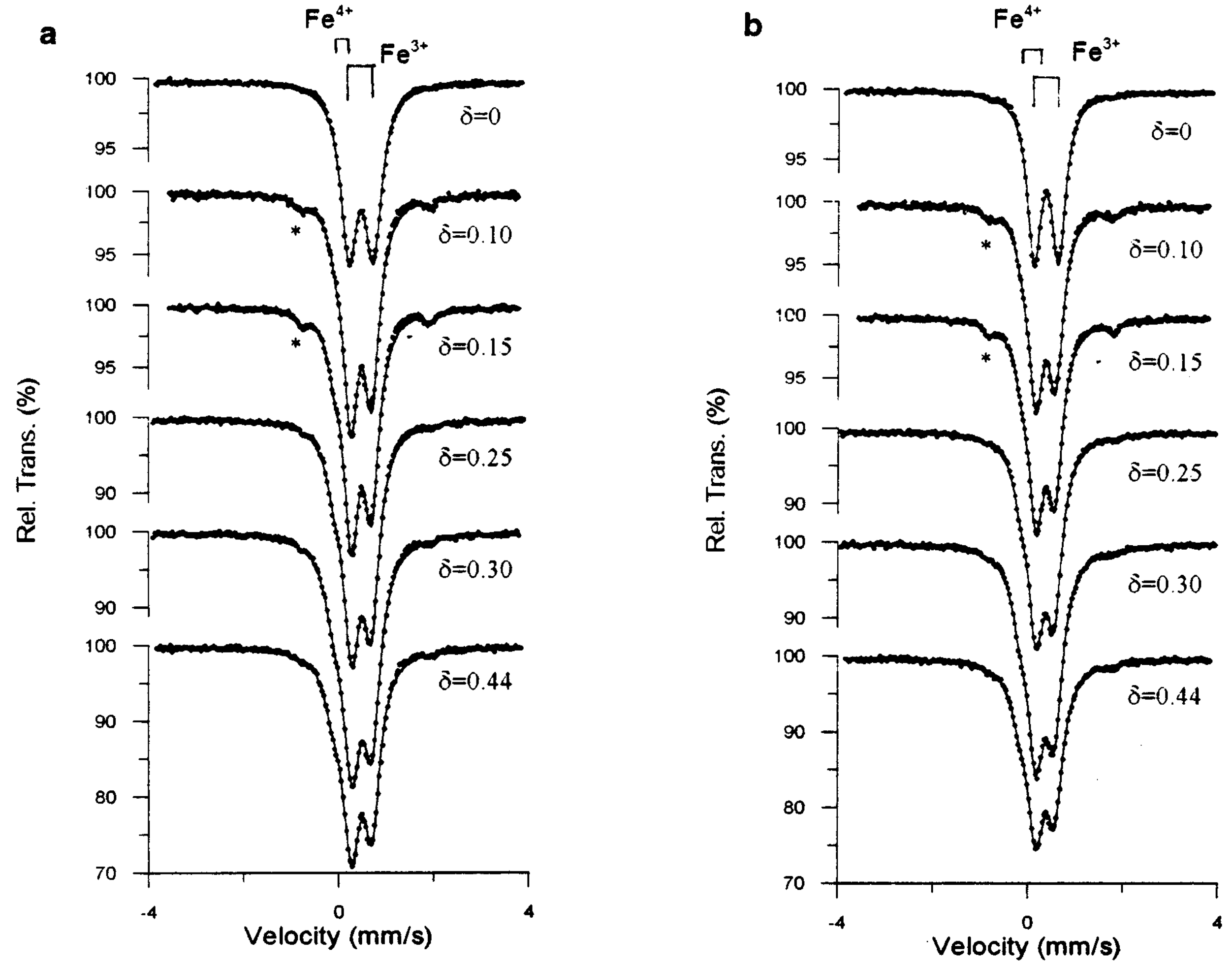

FIG. 3. (a) Room temperature and (b) 77 K Mössbauer spectra of $Na_{0.875-\delta}Fe_{0.875}Ti_{1.125}O_4$ ($\delta = 0, 0.10, 0.15, 0.25, 0.30$, and 0.44). The asterisks indicate the inner lines of α-Fe_2O_3 present in the $\delta = 0.10$ and 0.15 samples.

The observed difference in Fe^{4+} concentration in the more oxidized species seems to indicate that a partial backreduction of further Fe^{4+} cations took place. We believe that the backreduction is induced by small amounts of water, which are still present in the solvent used for the extraction reaction after distillation or during sample handling in air when the sample holder was loaded. An electrochemical study of the parent compound showed that the initial open-circuit voltage E (at zero current) progressively increases with sodium extraction (5). E increases from 0.1 V vs SHE in the starting material to 0.8 V in a sample with $\delta \approx 0.15$. Taking into account the standard electrode potential of water, E^0 $(\frac{1}{2}O_2/H_2O) = 1.23$ V, we expect that at high Fe^{4+} concentrations the oxidation of water will take place, $H_2O \rightarrow \frac{1}{2}O_2 + 2e^- + 2H^+$, and further Fe^{4+}, which was formed during the extraction process, will be backreduced, $Fe^{4+} + e^- \rightarrow Fe^{3+}$.

By linear extrapolation of the potentials at zero current of cells having positive electrodes at different sodium concentrations, the limiting electrode potential for water oxidation will be reached at $\delta \approx 0.20$. This value is in good agreement with the value we obtained at the crossover of curves 1 and 2 ($\delta = 0.19$) in Fig. 4. The more oxidized samples ($\delta = 0.25$, 0.30, and 0.44) would have an even greater oxidative potential. This explains the deviation of the observed from the expected Fe^{4+}/Fe^{3+} ratio for $\delta > 0.15$ and why a practically constant and low Fe^{4+} concentration is found in the more oxidized samples. Obviously, the backreduction of Fe^{4+} to Fe^{3+} should be accompanied by the incorporation of protons into the framework structure.

Up to 50% of the sodium can be extracted from the layered compound α-$NaFeO_2$ (12), and no deviation of the experimental Fe^{4+}/Fe^{3+} ratio obtained from Mössbauer spectroscopy was observed in any case. This is not surprising, because in α-$NaFeO_2$ sodium is extracted at a lower average potential ($E \approx 0.9$ V vs SHE, $< E^0(H_2O/\frac{1}{2}O_2)$), and water was not expected to be oxidized nor was Fe^{4+} expected to be backreduced to Fe^{3+}.

TABLE 2
Mössbauer Data and Fe^{3+}/Fe^{4+} Ratios Calculated from Mössbauer and ICP Data for the Series $Na_{0.875-\delta}Fe_{0.875}Ti_{1.125}O_4$

		Fe^{3+}			Fe^{4+}		
δ[a]	Temp	IS (mm/s)[b]	QS (mm/s)[c]	%	IS (mm/s)[b]	QS (mm/s)[c]	%
0	RT	0.371	0.515	100	—	—	0
	77 K	0.482	0.514		—	—	
0.10	RT	0.360	0.439	90	0.071	0.365	10
	77 K	0.484	0.427		0.095	0.284	
0.15	RT	0.359	0.414	85	0.075	0.406	15
	77 K	0.489	0.414		0.057	0.282	
0.25	RT	0.358	0.410	81	0.083	0.467	19
	77 K	0.492	0.399		0.022	0.247	
0.30	RT	0.360	0.424	79	0.070	0.474	21
	77 K	0.495	0.409		– 0.009	0.233	
0.44	RT	0.360	0.428	81	0.052	0.459	19
	77 K	0.492	0.419		– 0.008	0.248	

[a] From ICP.
[b] $\Delta IS = \pm 0.002$ mm/s for all values.
[c] $\Delta QS = \pm 0.004$ mm/s for all values.

Magnetic measurements. The magnetic susceptibility of an oxidized compound with $\delta = 0.15$ was measured between 4.2 and 300 K. The nonoxidized compound $Na_{0.875}Fe_{0.875}Ti_{1.125}O_4$ was also measured, since, to our knowledge, magnetic studies of this compound had not previously been reported. The decrease in magnetic moment observed in the sodium-extracted sample ($\delta = 0.15$, Fig. 5) is in agreement with the partial oxidation of Fe^{3+} to Fe^{4+} on sodium extraction. The amounts of Fe^{4+}, which can be calculated from this decrease in magnetic moments (10.7% for $\delta = 0.10$), agree fairly well with those we have obtained from ICP spectroscopy and Mössbauer spectroscopy (11.4 and 10%, respectively). The initial sample ($\delta = 0$) shows the paramagnetic behavior of the Fe^{3+} ions. The Curie–Weiss relationship $X_{\mathrm{mol}} = C/(T - \theta)$ is obeyed from 300 to 70 K. The magnetic moment observed in this temperature range, $\mu_{\mathrm{eff}} = 4.94\ \mu_{\mathrm{B}}$, is lower than the value calculated for 87.5% occupation of this ion per formula, $\mu = 5.53\ \mu_{\mathrm{B}}$. Furthermore, a certain field dependence of the magnetization of the nonoxidized sample, $\delta = 0$ (Fig. 6), seems to indicate a possible antiferromagnetic contribution. We will discuss here the contributions of possible interactions as explanations for the reduced paramagnetism of the parent compound. In this compound, the *M*1–*M*1 and *M*2–*M*2 separations are greater than the critical distance, 2.93 Å, for direct Fe^{3+}–Fe^{3+} *d*-orbital overlap (16). As occurs in the structures of $NaSc_{0.5}Fe_{0.5}TiO_4$ (17) and $NaFeTi_3O_8$ (18), an antiferromagnetic superexchange coupling between Fe^{3+} through oxygen atoms could also be present in $Na_{0.875}Fe_{0.875}Ti_{1.125}O_4$ as a consequence of the bulk concentration of Fe^{3+}. The effect of statistically distributed ions could explain why the Néel temperature is not reached.

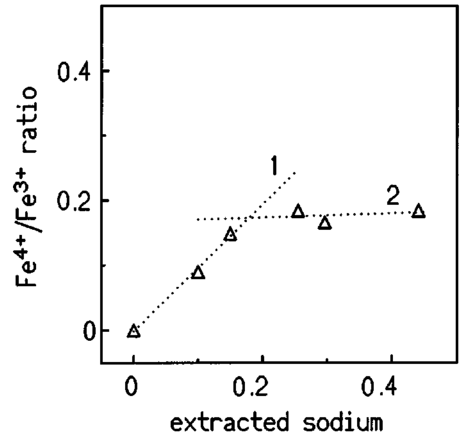

FIG. 4. Observed Fe^{4+}/Fe^{3+} ratios deduced from Mössbauer spectroscopy as a function of the extracted sodium (δ). Curves 1 and 2 have been fitted to data points in the range $0 \leq \delta \leq 0.15$ and $0.25 \leq \delta \leq 0.44$, respectively.

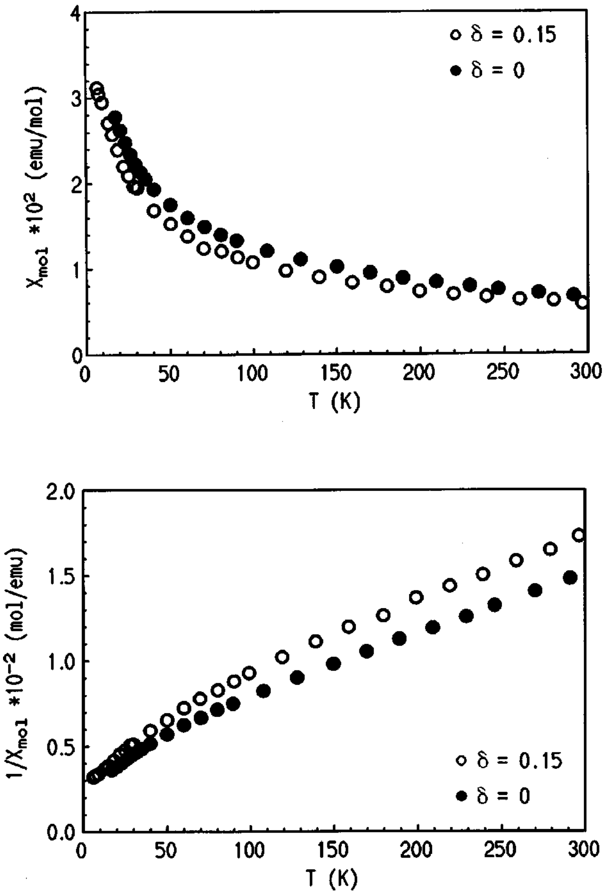

FIG. 5. Magnetic susceptibility of $Na_{0.875-\delta}Fe_{0.875}Ti_{1.125}O_4$ ($\delta = 0$ and 0.15) and the corresponding slopes $1/X$ as function of temperature.

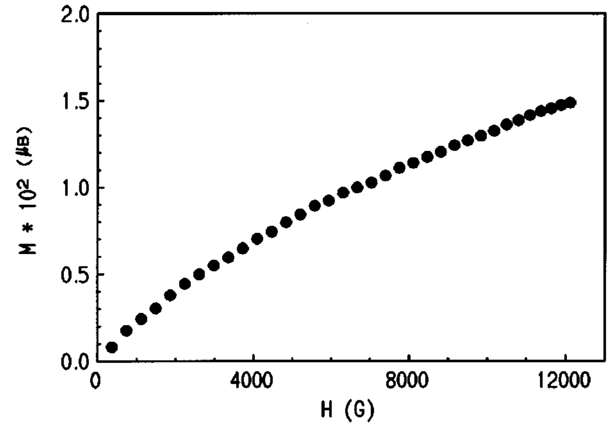

FIG. 6. Magnetization of $Na_{0.875}Fe_{0.875}Ti_{1.125}O_4$ as function of the magnetic field.

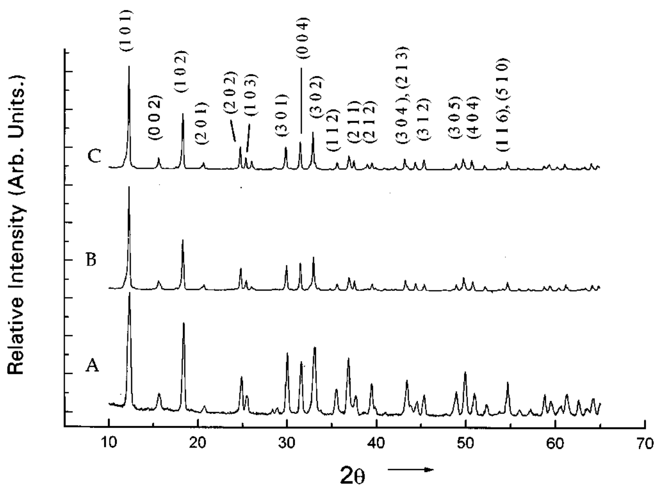

FIG. 7. Powder X-ray diffractograms of $Na_{0.875-\delta}Fe_{0.875}Ti_{1.125}O_4$. (A) $\delta = 0.10$, (B) $\delta = 0.26$, (C) $\delta = 0.44$.

Explanation of the magnetic behavior in the parent structure is complicated by the relatively complex boundaries (a quadruple ribbon of edge-shared octahedra, which is further corner-shared to four other ribbons; all are edge-shared along the b axis), leading to M–O–M angles more favorable to superexchange, 126° between two quadruple-rutile chains (O1-shared octahedras) and 157° in a quadruple chain between edge-shared octahedra (M1–O4–M2), than those in the planes perpendicular to them, $\approx 90°$ between edge-shared octahedra in the parent compound. Below ≈ 70 K, the plot of $1/X_{\mathrm{mol}}$ vs T deviates from linearity for all compositions, as expected from the relatively high Weiss constant ($\theta = 120$ K), which is surprisingly close to the values observed for the structurally different compounds $NaSc_{0.5}Fe_{0.5}TiO_4$ (17) and $NaFeTi_3O_8$ (18). A similar interaction mechanism can then be assumed for $Na_{0.875}Fe_{0.875}Ti_{1.125}O_4$.

X-ray diffraction. The lattice parameters for the nonoxidized $Na_{0.875}Fe_{0.875}Ti_{1.125}O_4$, determined by a least-squares refinement using powder data, are $a = 9.264(3)$ Å, $b = 2.971(1)$ Å, $c = 11.353(3)$ Å, and $V = 312.5(2)$ Å^3. These values are consistent with the literature (1). With respect to the oxidized phases, the XRD patterns are similar and easily related to the parent phase (Fig. 7). This indicates that oxidation occurred through a topotactic reaction as usually happens in low-temperature extraction reactions. However, the variation in lattice parameters does not follow a simple rule. The expectation of decreased volume with sodium removal is not clearly fulfilled, as can be deduced from data plotted in Fig. 8. The a lattice parameter increases almost linearly with decreasing sodium content, while the b lattice parameter decreases only slightly. On the other hand, the c lattice parameter initially increases with decreasing Na content (up to 0.64 Na per formula) and then decreases with further sodium extraction. The unit cell volume remains practically constant during the Na extraction due to the combined effects of these different trends. Rietveld structural refinements of the extracted phases $Na_{0.875-\delta}Fe_{0.875}Ti_{1.125}O_4$ in the whole range of sodium nonstoichiometry

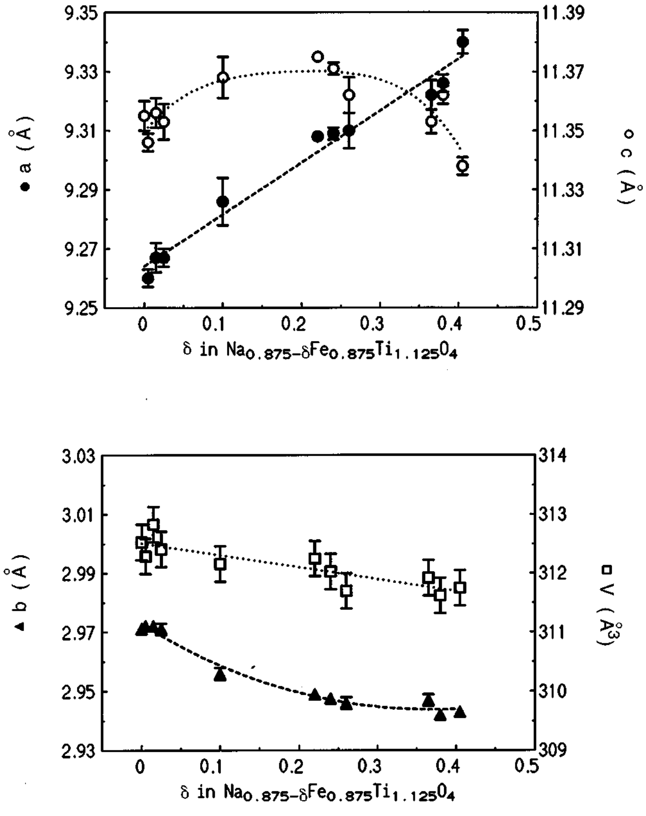

FIG. 8. Evolution of cell parameters a, b, and c and cell volume V as a function of extracted sodium, δ in $Na_{0.875-\delta}Fe_{0.875}Ti_{1.125}O_4$.

($0 \leq \delta \leq 0.44$) were undertaken to study the origin of such cell parameter variation. The oxidation of the parent compound is accompanied by a broadening of reflections (evident in a continuous increase in FWHM parameters u, v, w) and a remarkable decrease in intensities. Structural refinements with the poorer powder data for the oxidized samples did not lead to reasonable refinements, e.g., in locating the exact positions of light atoms, such as oxygen or sodium. Therefore, we reported the oxidation procedure for single crystals of the initial composition $Na_{0.79}Fe_{0.79}Ti_{1.21}O_{4.0}$ and crystal data in an earlier paper (15).

Each sodium atom is coordinated by six nearest-neighbor oxygen atoms in a trigonal prismatic environment. Three additional oxygen atoms are located out from the three prism faces. The prisms share faces along the tunnel axis. When sodium is extracted, a slight but significant rearrangement of the structure takes place. It is clear that the elimination of some Na ion (up to 38% in single crystal) and the concomitant increase in Fe^{4+} concentration will shorten, by covalency, the M–O distance. The average $M(1)$–O and $M(2)$–O distances are 1.998 and 1.988Å in the starting material and 1.989 and 1.984 Å in the most oxidized crystal (Table 3). As a result of the shorter M–O distance, the average Na–O distance increases by 0.027 Å (from 2.780 to 2.807 Å, Table 3). One zig-zag group consists of $M(1)O_6$ and $M(2)O_6$ octahedra. The differences between the average $M(1)$–O and $M(2)$–O distances in the unoxidized crystal are clearly smaller ($\approx$0.01 Å) than the differences in the effective ionic radii (0.04 Å) between Fe^{3+}_{VI} (0.645 Å) and Ti^{4+}_{VI} (0.605 Å) (19). They are independent of the degree of sodium extraction; i.e., they do not depend on the amount of tetravalent iron present in the structure. This suggests that Fe^{3+}/Fe^{4+} and Ti^{4+} cations are randomly distributed over the two sets of octahedral sites in both the initial and the oxidized samples.

The shortening of the $\underline{b}$ axis (by 0.024 Å) is a consequence of a decrease in the distances between $M(1)$–O(1), $M(1)$–O(4′), $M(2)$–O(2), and $M(2)$–O(3′). On the other hand, the increase in the distance between $M(2)$ and the apical oxygen atom O(4′) (Table 3) is responsible for the increase in both the $\underline{a}$ and the $\underline{c}$ axis (0.052 and 0.067 Å, respectively). The shift vector of the apical oxygen atom away from the metal center is not exactly parallel to the (1 0 1) plane, but contains some contribution of the $\underline{a}$ axis. This explains why both $\underline{a}$ and $\underline{c}$ parameters initially increase (observed in both single crystals and powder samples), whereas further oxidation of the framework structure (only reached with powder samples) causes a return of the $\underline{a}$ axis length.

With decreasing sodium content, the sodium atoms tend to shift away from the center of the double tunnels (or away from the sharp angle formed by interconnection of quadruple blocks) toward the oxygen atom O4 (toward the obtuse O1–O4–O2 angle; see Fig. 9).

These atomic positional changes with decreasing sodium content are continuous and can be readily explained by the presence of overwritten quadruple-rutile chains around the origin of the $Na_{0.79-\delta}Fe_{0.79}Ti_{1.21}O_4$ structure. The positional shift of each atom with decreasing Na content is indicated by arrows in Fig. 9.

TABLE 3
Selected Interatomic Distances (Å) for $Na_{0.79-\delta}Fe_{0.79}Ti_{1.21}O_4$ with $\delta = 0$ (A) and $\delta = 0.30$ (B) from Ref. (15)

Crystal	A	B
	$M(1)$ Octahedron	
$M(1)$–$O(1)_{eq}$ (2×)	1.937(5)	1.928(7)
–$O(4')_{eq}$ (2×)	2.092(5)	2.078(7)
–$O(3')_{ap}$ (1×)	1.925(8)	1.93(1)
–$O(4')_{ap}$ (1×)	2.006(7)	1.99(1)
Average $M(1)$–O	1.998	1.988
	$M(2)$ Octahedron	
$M(2)$–$O(2)_{eq}$ (2×)	1.921(5)	1.910(7)
–$O(3)_{eq}$ (2×)	2.050(5)	2.028(8)
–$O(1)_{ap}$ (1×)	1.982(7)	1.98(1)
–$O(4)_{ap}$ (1×)	2.013(7)	2.05(1)
Average $M(2)$–O	1.989	1.984
	Na–O polyhedron	
Na–O(1) (1×)	2.64(1)	2.70(2)
–O(2′) (2×)	2.599(9)	2.61(2)
–O(2″) (1×)	2.29(1)	2.26(2)
–O(3) (2×)	2.399(8)	2.46(2)
–O(1′) (1×)	3.16(1)	3.22(2)
–O(4″) (2×)	3.47(1)	3.47(2)
Average Na–O	2.780	2.807

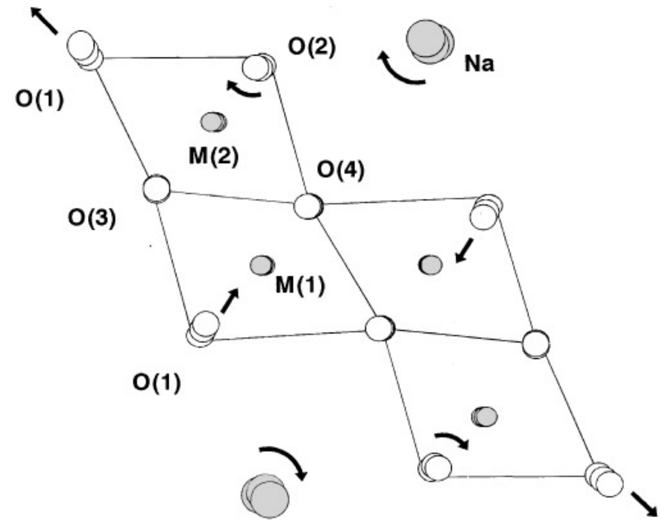

FIG. 9. The continuous change in the quadruple-rutile framework with decreasing Na content from 0.79 to 0.49 in $Na_{0.79-\delta}Fe_{0.79}Ti_{1.21}O_4$ along the $\underline{b}$ axis. The positional shifts of atoms around the screw axis, together with decreasing sodium content, are indicated by arrows.

TABLE 4
Isotropic and Anisotropic Temperature Factors[a] ($\beta \times 10^3$) for $Na_{x-\delta}Fe_xTi_{2-x}O_4$ from Ref. (15)

δ	Occ.	B_{eq} (Å)	β_{11}	β_{22}	β_{33}	β_{13}
0	0.79(2)	2.9(2)	34(4)	65(7)	11(3)	6(3)
0.19	0.60(2)	5.6(5)	25(6)	177(18)	16(5)	8(4)
0.30	0.49(2)	5.6(5)	15(7)	171(28)	29(8)	10(6)

[a] $\beta_{12} = \beta_{23} = 0$.

Furthermore, the large amplitude of the thermal vibration of sodium ions along the *b* direction that was observed is related to a relatively unhindered vibration of sodium atoms along the tunnel. The partial removal of sodium can be expected to facilitate the mobility of the remaining sodium ions. Thus, larger values of β_{22} are expected in the more extracted materials. The large values of β_{22} in Table 4 seem to reinforce this hypothesis. In the compound $Na_xTi_2O_4$ ($x \approx 0.57$) (4), which is isostructural with the title material, the sodium cations occupy two different positions separated along y by $\frac{1}{2}b$ with similar population factors (0.3 and 0.27). However, the splitting of the sodium atoms into two positions similar to those proposed (4) did not lead to an improvement in the refinements. In this context, it is worth recalling that we introduced sodium deficiency with a room-temperature extraction procedure, while Akimoto *et al.* grew their single crystals at high temperature. Although the splitting of the unique sodium position could be a more stable situation, the migration of a portion of the sodium ions obviously does not occur at room temperature. This is another example of the obtention of metastable phases with soft-chemistry routes.

CONCLUSIONS

The chemical sodium extraction reaction in $Na_{0.875}Fe_{0.875}Ti_{1.125}O_4$ proceeds topotactically and leads to a new series of nonstoichiometric compounds that possess double tunnels with a highly nonstoichiometric occupation by sodium atoms. For the first time, we were able to prepare a rutile-related oxide containing an appreciable number of unstable Fe^{4+} cations.

The presence of Fe^{4+} was confirmed by both Mössbauer spectroscopy and magnetic measurements. Furthermore, the chemical composition obtained from ICP spectroscopy was corroborated in the range $0 \leq \delta \leq 0.15$ by the Fe^{3+}/Fe^{4+} ratios, which were deduced from Mössbauer spectroscopy and magnetic measurements. On further sodium extraction the amount of Fe^{4+} did not increase. The deviation from the expected Fe^{4+}/Fe^{3+} ratio was explained in terms of a subsequent backreduction of further Fe^{4+}, which was generated during the extraction procedure.

The sodium extraction led to a significant increase in one of the apical metal–oxygen distances in both types of octahedra, explaining the increase in both $\underline{a}$ and $\underline{c}$ parameters with sodium removal. On the other hand, the decrease in the equatorial metal–oxygen distances in both types of octahedra causes shortening of the tunnel $\underline{b}$ axis with sodium extraction.

With the procedure described, no more than 0.44 Na^+/formula, i.e., 50% of the initial sodium, could be extracted. This value, $\delta = 0.44$, seems then to be the limit of sodium extraction for the NO_2BF_4 oxidation agent. Our final goal, the preparation of the pseudo-binary oxide $Fe_{0.875}Ti_{1.125}O_4$, should be feasible when stronger chemical oxidants and/or prolonged reaction times and treatments with the same oxidizing agent are employed.

ACKNOWLEDGMENTS

We thank CICYT (Project MAT 92/0374, MAT 95/0809, and MAT 96/1588/E) for financial support. The DAAD, the Spanish Ministry of Foreign Affairs, and the Land Baden–Württemberg are also acknowledged for providing a fellowship to A. Kuhn.

REFERENCES

1. W. G. Mumme and A. F. Reid, *Acta Crystallogr. B* **24,** 625 (1968).
2. F. Archaimbault, P. Odier, and J. Choisnet, *Solid State Ionics* **28/30,** 1357 (1988).
3. F. Archaimbault and J. Choisnet, *J. Solid State Chem.* **90,** 216 (1991).
4. Y. Akimoto and H. Takei, *J. Solid State Chem.* **90,** 92 (1991).
5. A. Kuhn, F. García-Alvarado, E. Morán, and M. A. Alario-Franco, *Mater. Res. Soc. Symp. Proc.* **369,** 481 (1995).
6. H. M. Rietveld, *Crystallogr.* **22,** 151 (1967); *J. Appl. Crystallogr.* **65,** 2 (1969).
7. J. Rodríguez-Carvajal, "FULLPROF: A Program for Rietveld Refinement and Pattern Matching Analysis," Abstract of the Satellite Meeting of the XVth Congress of the International Union of Crystallography, Toulouse, France, 1992, p. 127.
8. R. A. Brand, *Nucl. Instrum. Methods Phys. Res. B* **28,** 398 (1987).
9. A. R. Wizansky, P. E. Rauch, and F. J. DiSalvo, *J. Solid State Chem.* **81,** 203 (1989).
10. Y. Takeda, S. Naka, M. Takano, T. Shinjo, T. Takada, and M. Shimada, *Mater. Res. Bull.* **13,** 61 (1978).
11. J. B. MacChesney, R. C. Sherwood, and J. F. Potter, *J. Chem. Phys.* **43,** 1907 (1965).
12. Y. Takeda, K. Nakahara, M. Nishijima, N. Imanishi, and O. Yamamoto, *Mater. Res. Bull.* **29,** 659 (1994).
13. J. P. Parant, R. Olazuaga, M. Devalette, C. Fouassier, and P. Hagenmuller, *J. Solid State Chem.* **3,** 1 (1971).
14. L. H. Bowen, *Ref. Data J.* **2,** 76 (1979).
15. A. Kuhn, F. García-Alvarado, E. Morán, M. A. Alario-Franco, and U. Amador-Elizondo, *Solid State Ionics* **86–88,** 811–818 (1996).
16. J. B. Goodenough, "Magnetism and the Chemical Bond," p. 266. Interscience, New York, 1963.
17. A. F. Reid and M. J. Sienko, *Inorg. Chem.* **6,** 321 (1967).
18. A. F. Reid, H. K. Perkins, and M. J. Sienko, *Inorg. Chem.* **7,** 119 (1968).
19. R. D. Shannon and C. Prewitt, *Acta. Crystallogr. B* **25,** 925 (1969).